

Galaxy Evolution

Impact of Redshift

k-corrections

Finding galaxies at large redshift

spectroscopic redshifts

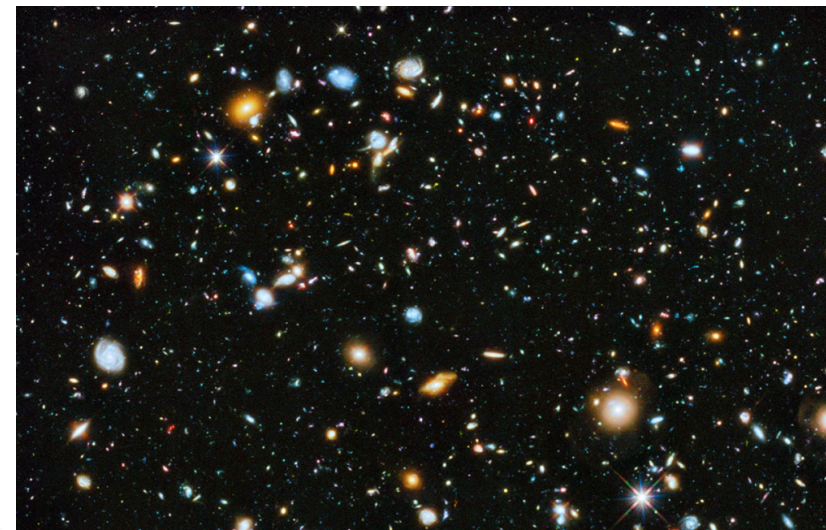
photometric redshifts

specialized techniques

Results

1

Galaxy Evolution: Use observations at higher z to track evolution of **population**



2

Practicalities

Requires significant samples with well-understood selection biases

Can only track population — no way to know for certain what the evolutionary endpoint will be.

Can use all the same techniques to estimate physical quantities...

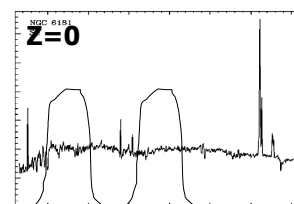
BUT, be aware that local calibrations may no longer apply in very different physical conditions!

Practicalities of dealing w/ redshift

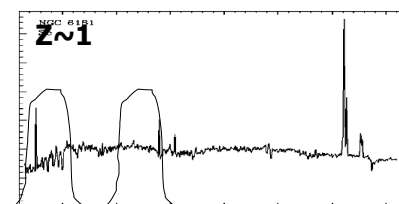
Galaxies are fainter: $D_L(z)^{-2}$

Surface brightnesses are dimmer: $[D_A(z)/D_L(z)]^2$

Observed wavelength \neq rest wavelength



$$\lambda_{\text{apparent}} \rightarrow \lambda_{\text{intrinsic}} (1+z)$$



Intrinsically bluer wavelengths appear in the filter

$$\Delta\lambda_{\text{apparent}} \rightarrow \Delta\lambda_{\text{intrinsic}} (1+z)$$

4

Same filter covers a smaller fraction of the spectrum

3

Even if spectrum is constant,
apparent color+magnitude change

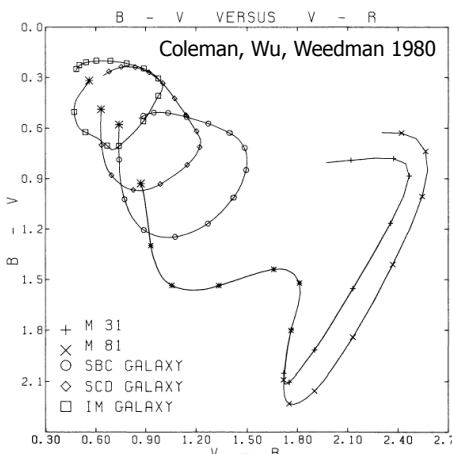


FIG. 12.— $B - V$ color vs. $V - R$ color for the five spectral energy distributions defined by Tables 2–5. Observational uncertainties are ± 0.1 to ± 0.2 mag; intrinsic differences among galaxies of the same type can be greater (see Figs. 14–20). Symbols occur at intervals of 0.1 in redshift.

5

Different intrinsic
spectra vary
differently with z

Strategies for constructing redshift-independent magnitudes:

Adjust choice of filters to compare
same rest-frame wavelengths (u at
 $z=0$, r at $z=1$)

Estimate underlying SED, and “k-
correct” magnitude to consistent
rest-frame wavelength

6

Definition of the “k-correction”

Consider a source observed to have apparent magnitude m_R when observed through photometric bandpass R , for which one wishes to know its absolute magnitude M_Q in emitted-frame bandpass Q . The K correction K_{QR} for this source is defined by

$$m_R = M_Q + DM + K_{QR}, \quad (2)$$

where DM is the distance modulus, defined by

$$DM = 5 \log_{10} \left[\frac{D_L}{10 \text{ pc}} \right], \quad (3)$$

where D_L is the luminosity distance (e.g., Hogg 1999) and 1 pc = 3.086×10^{16} m.

Hogg et al 2002; astro-ph/0210394

Note: There are other definitions floating around. A common one has a factor of $(1+z)$ taken out, to account for the bandpass stretching, which is independent of the shape of the underlying spectrum

$$k_B(z) = B(z) - B(z=0) - 2.5 \log(1+z). \quad \text{Frei & Gunn 1994}$$

Different underlying spectra will have
different k-corrections, in different filters, at
different redshifts

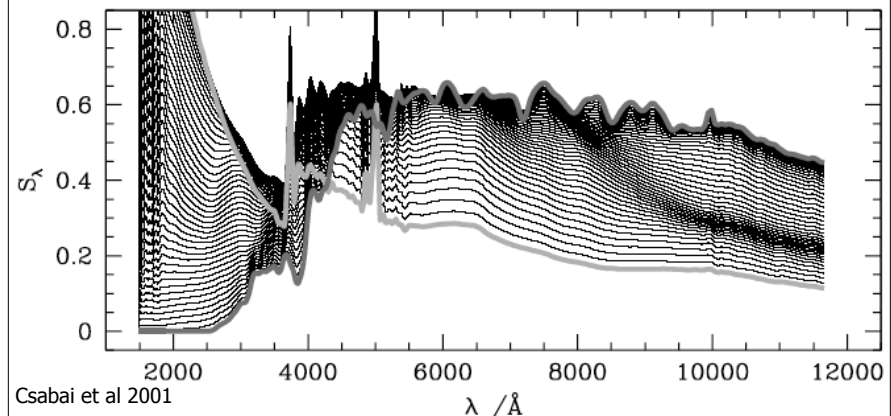


Fig. 12.— Illustration of the 1D type manifold. A few SEDs are plotted here for a equally spaced type parameter values. The reddest and bluest SEDs are shown with the thick dark and light grey curves, respectively.

7

k-corrections:

Usually make galaxies fainter than expected

Most spectra fall towards UV, so looking at dimmer part of spectra

Corrections smaller and less variable in NIR

Power-law side of stellar black bodies

Depends on dust

Anything that affects the spectrum changes the k-correction

Can be negative in the submillimeter

Peak of cool dust black-body moves into band-pass.

Finding Redshifted Galaxies

Brute force — measure lots of redshifts

Photometric redshifts

galaxies

QSO's

including dust+IGM absorption

Selecting high-z galaxies

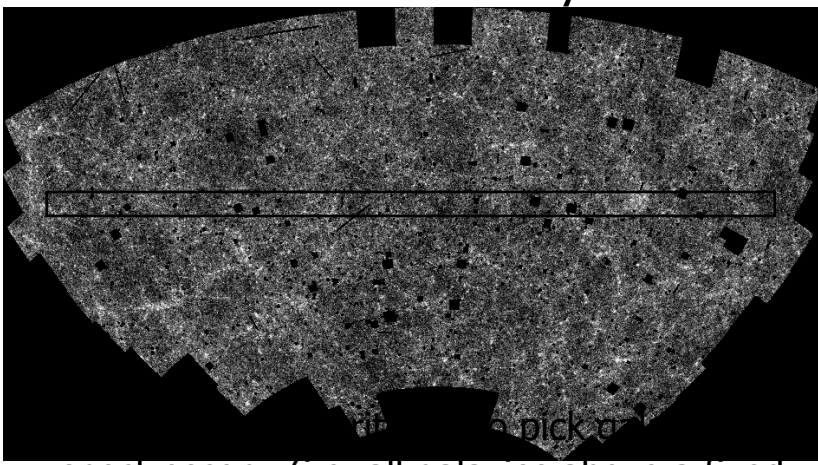
Dropout techniques ("Lyman Break Galaxies"=LBG)

Selecting non-SF galaxies (NIR, BzK)

Lyman-alpha emitters

10

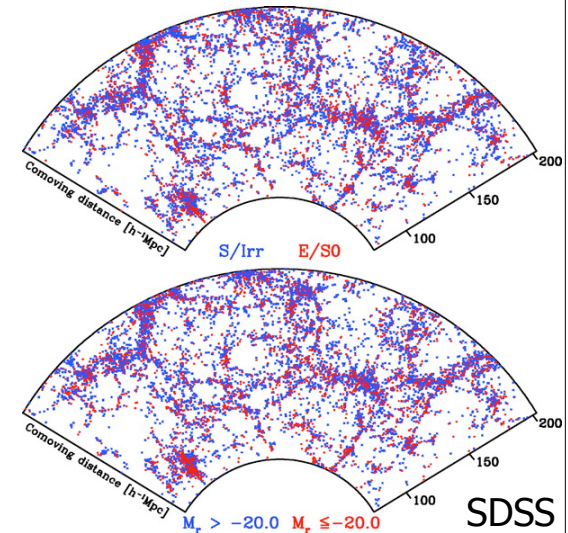
Brute force spectroscopy: "redshift surveys"



11 magnitude in some filter, in some area of the sky)

Redshift surveys: Probe galaxy population and clustering simultaneously

Morphology:
Ellipticals more clustered



Mass:
Fainter galaxies less clustered

12

"Photometric Redshifts" (or "photo-z's"): Fit the observed data with redshifted SED

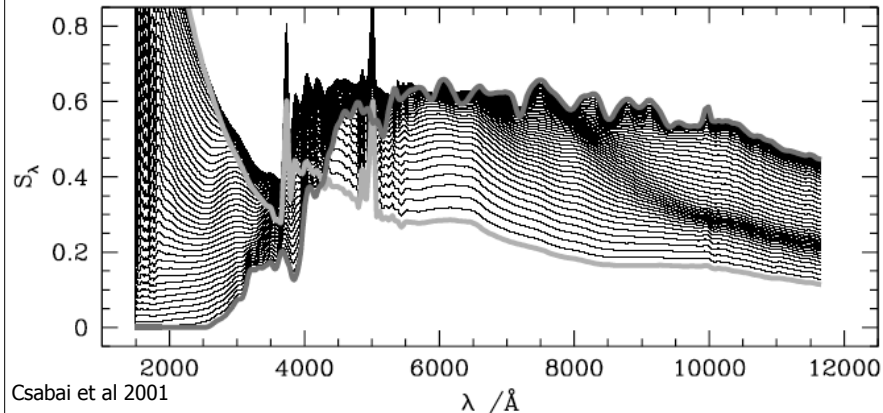
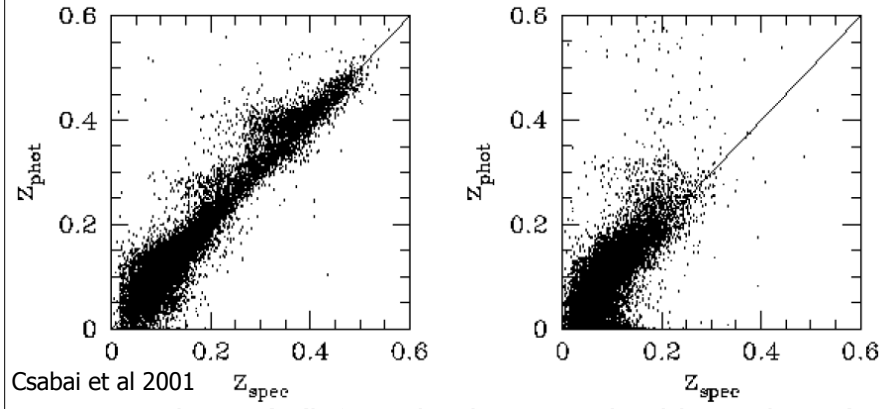


Fig. 12.— Illustration of the 1D type manifold. A few SEDs are plotted here for a equally spaced type parameter values. The reddest and bluest SEDs are shown with the thick dark and light grey curves, respectively.

Photo-z's are good to ~ 0.1 , with some catastrophic failures



SDSS Photo-z's (left: red galaxies; right: blue galaxies)
(Failures can be catastrophic though -- errors are non-Gaussian.
For wider ranges in z , NIR usually required for accuracy)

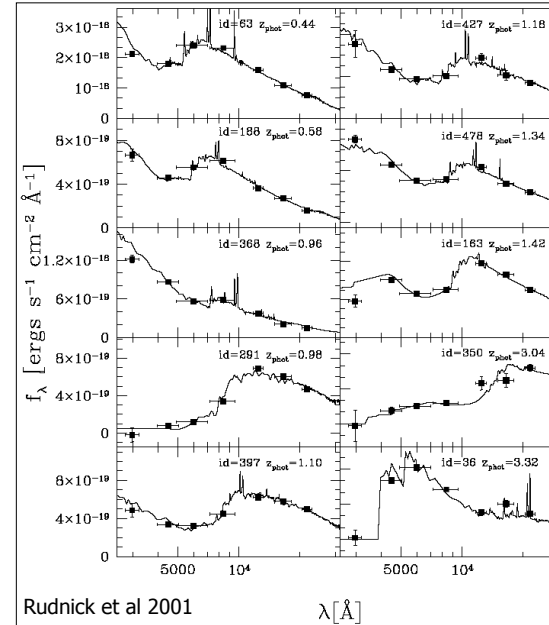
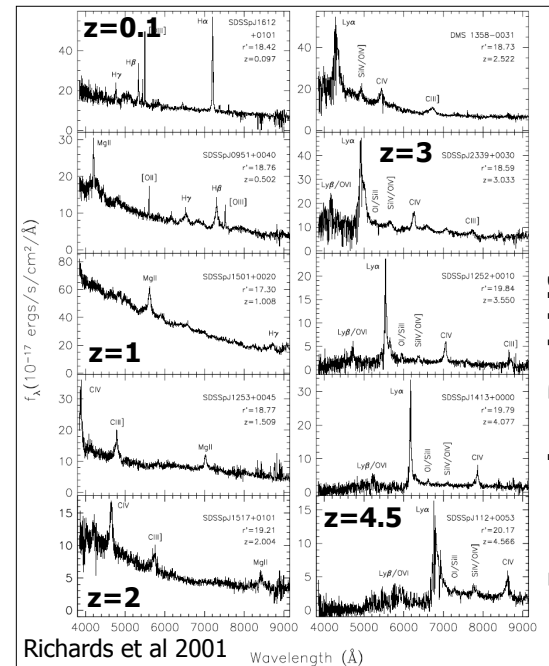


FIG. 5.— Sample of template fits to photometric data for 10 objects in the HDF-S. The measured z_{phot} increases down and to the right. In addition to blue, star-forming galaxies, there are many galaxies at $z > 1$ with strong Balmer or 4000 Å breaks.

Take a wide range of filters (UV-NIR best) and fit the observed SED with redshifted template spectra
Template also constrains:
SFR
Stellar Mass Extinction

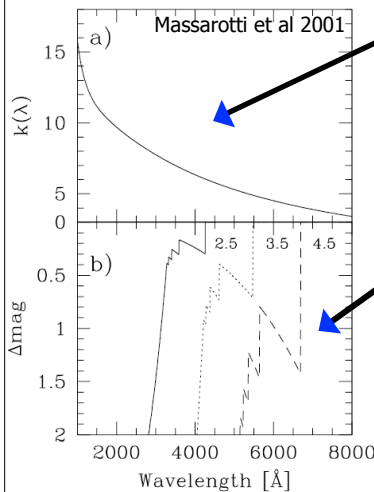
Photo-z's for QSOs: Get z and classification



← Increasing Redshift

Lyα is strongest line and moves into the optical at $z \sim 2.5$

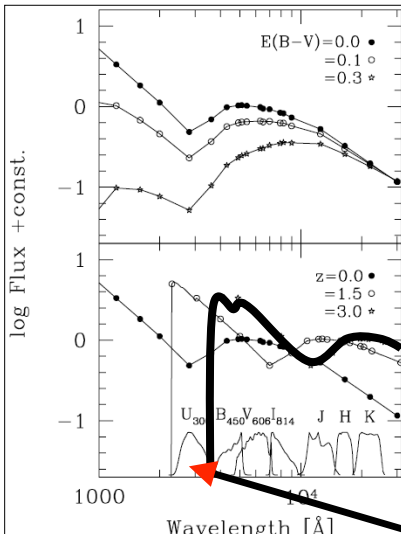
Photo-z's: Need to include dust + IGM



Dust: probably increasingly important at higher z , where a larger fraction of galaxies seem to be in the "starburst" (i.e. ULIRG) mode, Metallicity lower, though.

IGM: Ly- α absorption from hydrogen along the line of sight to the distant galaxy produces sharp "breaks" in the spectra, and absorbs all photons bluer than a certain wavelength

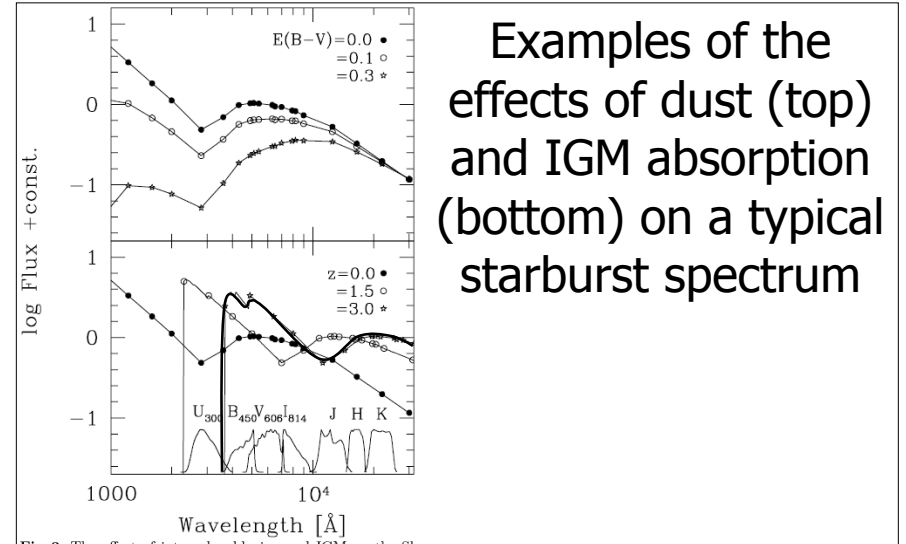
Fig. 2. Panel a) the adopted dust attenuation law after Calzetti (1999). Panel b) the IGM attenuation in a magnitude scale at redshift 2.5, 3.5 and 4.5, as labelled, according to Madau (1995)



"Lyman Break Technique": Use feature produced by IGM Ly α absorption to identify high- z galaxies

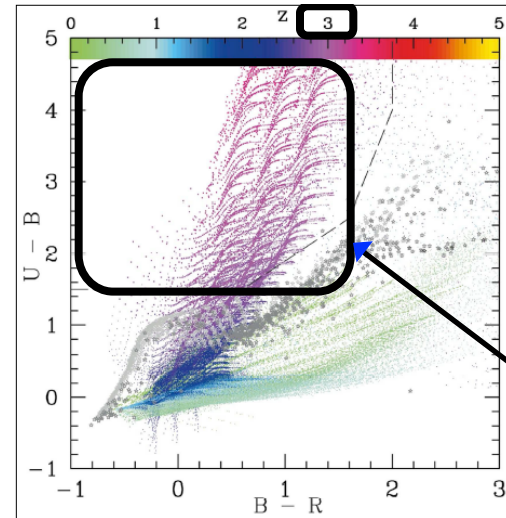
No flux in U-band: "U band drop out"

Fig. 3. The effect of internal reddening and IGM on the Sb reference template from Buzzoni (2000). Dust attenuation for $E(B - V)$ up to 0.3 mag, as labelled, is shown in the upper panel, while the expected break induced by the Ly- α forest at $z = 1.5$ and $z = 3$ is shown in the lower panel. For reference, the HST photometric system and the Johnson JHK bands are displayed at the bottom



Examples of the effects of dust (top) and IGM absorption (bottom) on a typical starburst spectrum

Fig. 3. The effect of internal reddening and IGM on the Sb reference template from Buzzoni (2000). Dust attenuation for $E(B - V)$ up to 0.3 mag, as labelled, is shown in the upper panel, while the expected break induced by the Ly- α forest at $z = 1.5$ and $z = 3$ is shown in the lower panel. For reference, the HST photometric system and the Johnson JHK bands are displayed at the bottom

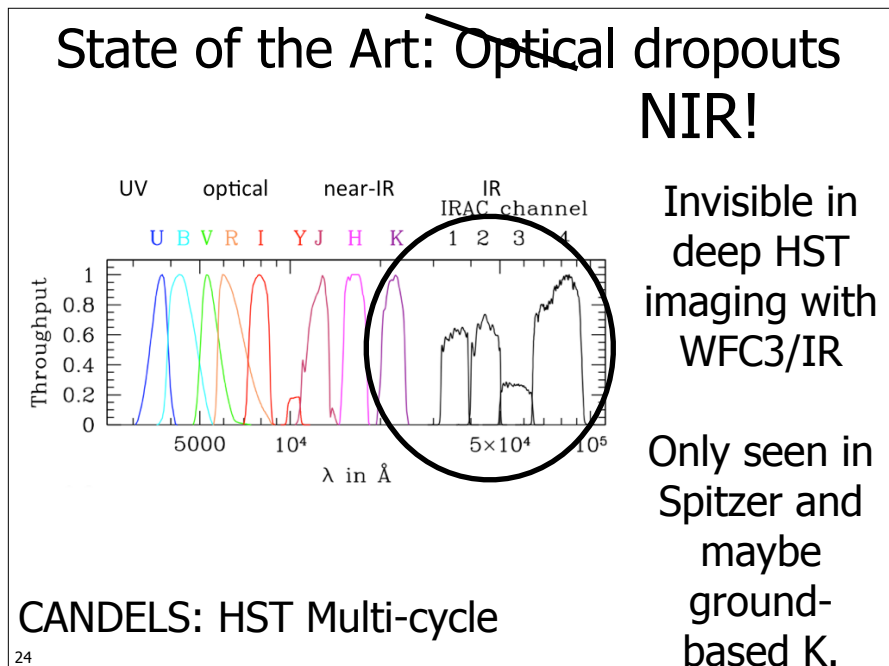
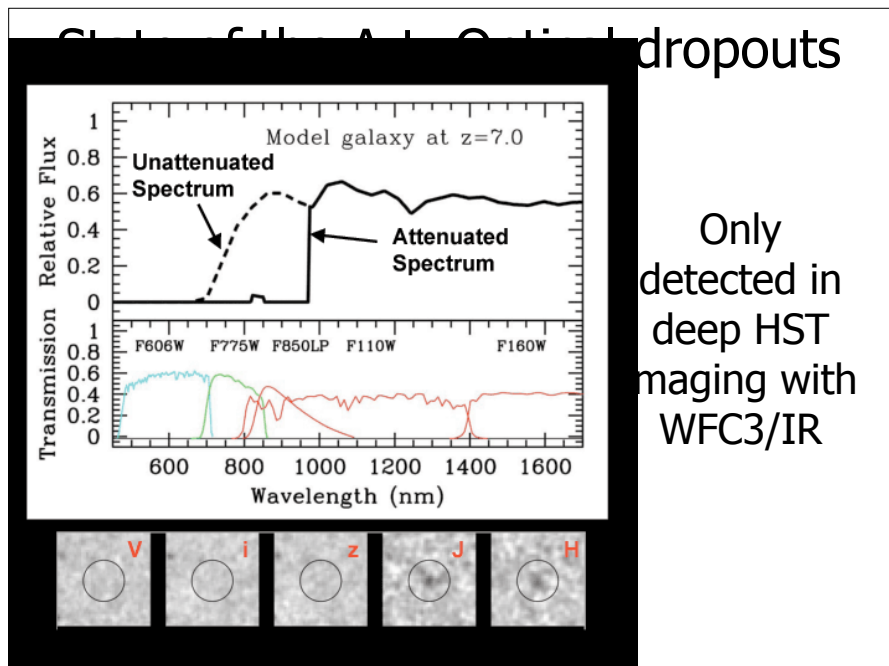
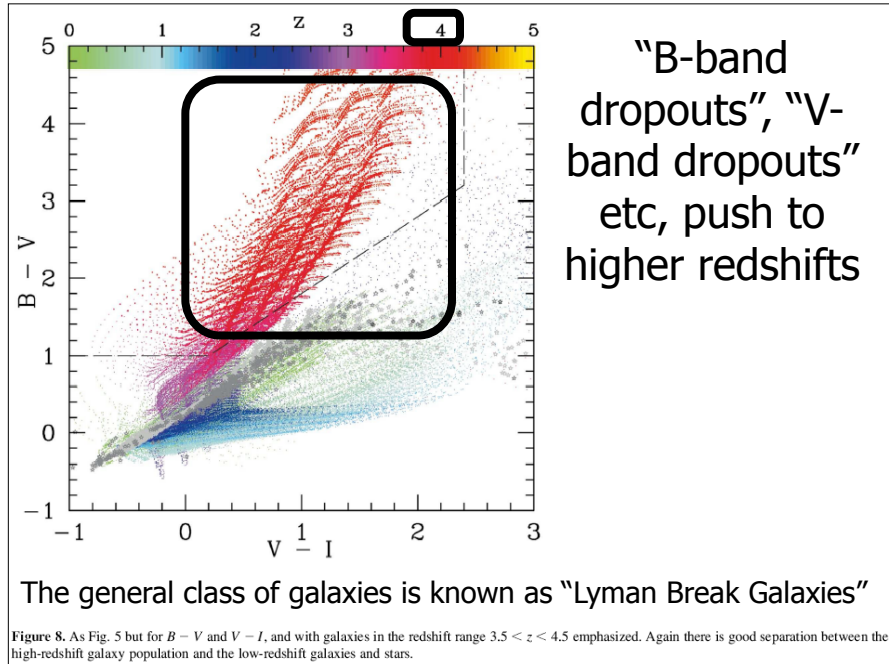
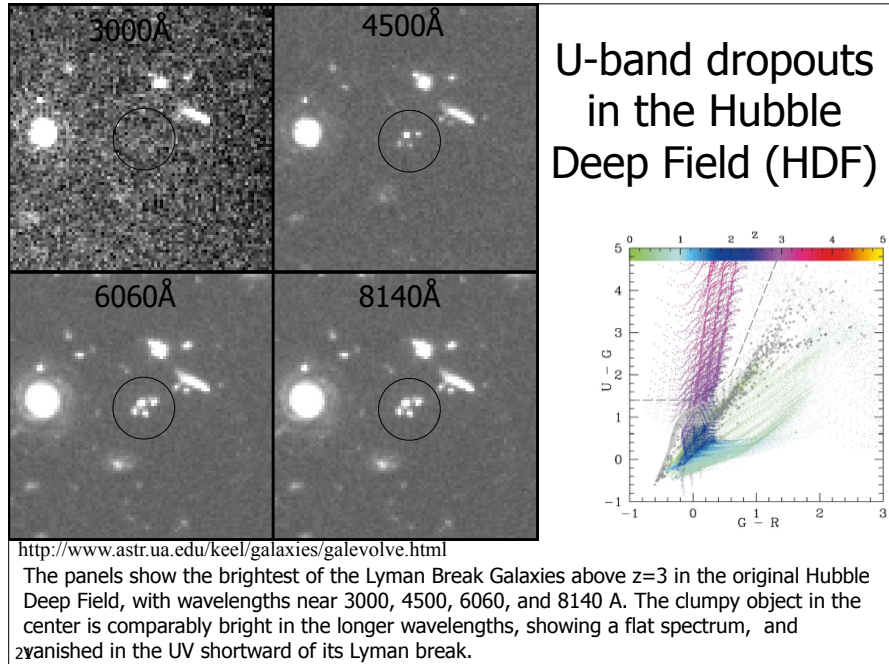


$z \sim 3$ galaxies are extremely red in U-B, solely due to IGM

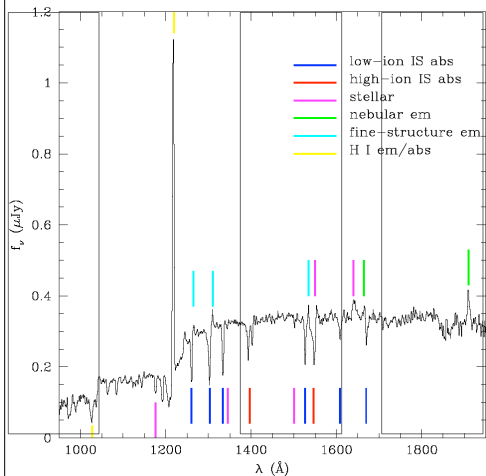
Few galactic stars or other galaxies fall in this color region.

Fig. 5. Variation of $U - B$ and $B - R$ colours with redshift z . Galaxies are indicated by small dots coloured by redshift: young (age < 100 Myr) galaxies in the redshift range $2.75 < z < 3.5$ have been emphasized. The colours of galactic stars have been superimposed: light grey stars are those from the model data of Bessell, Castelli & Plez (1998), while the darker grey stars are from the photometric standards of Landolt (1992). Black stars represent M dwarfs and use data obtained from Bessell (1991) and Leggett (1992). Our selection criteria are indicated by the dashed lines. A broad area of colour-colour space is enclosed, allowing for efficient selection of candidate high-redshift galaxies in spite of photometric errors, as long as a sufficiently large break in $U - B$ can be observed. In practice this is the limiting factor, owing to the relatively poor quantum efficiency U of the TEK CCDs used compared with that of more modern detectors. Galaxies at redshifts above $z \approx 3.5$ will have almost complete absorption in U and thus extreme $U - B$ colours off the top of this plot, but in practice we will only measure lower limits to this colour. As redshift increases, increasing absorption in B will push $B - R$ further towards the red. Making the upper bound to the cut in $B - R$ (or more generally for the two longer wavelength bandpasses) further to the red allows for selection of objects at higher redshifts than are shown on this plot, however this must not be pushed so far as to reach the stellar locus.

Stevens & Lacy 2001



LBG: All star forming, by construction



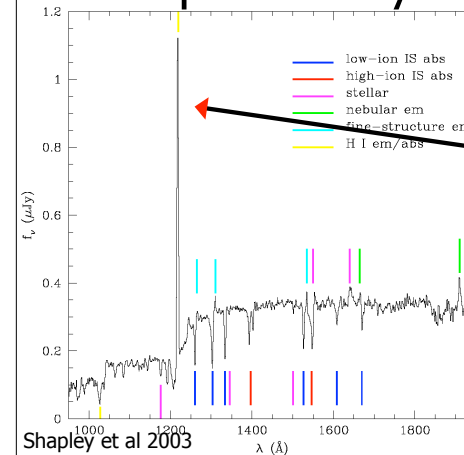
**Significant UV flux
(1300-2000Å)
= O-stars**

Rest-frame UV spectrum of coadded Lyman Break Galaxies (LBG) at $z \sim 3$

- Strong Ly α emission
- Blue trough shortward of Ly α = galactic-wide outflow?

FIG. 2. — A composite rest-frame UV spectrum constructed from 811 individual LBG spectra. Dominated by the emission from massive O and B stars, the overall shape of the UV continuum is modified shortward of Ly α by a decrement due to inter-galactic HI absorption. Several different sets of UV features are marked: stellar photospheric and wind, interstellar low- and high-ionization absorption, nebular emission from H II regions, Si II* fine-structure emission whose origin is ambiguous, and emission and absorption due to interstellar HI (Ly α and Ly β). There are numerous weak features which are not marked, as well as several features bluewards of Ly α which only become visible by averaging over many sightlines through the IGM. The composite LBG spectrum is available in electronic form from <http://www.astro.caltech.edu/~aes/lbgspec/>.

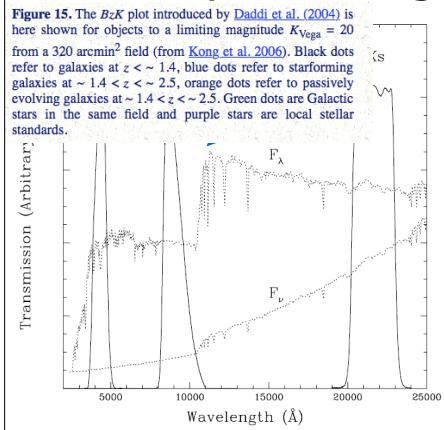
Ly α Emitters: Selects SF galaxies, but potentially to lower SFRs



Select using
narrow band
filters targeting
specific
redshift

FIG. 2. — A composite rest-frame UV spectrum constructed from 811 individual LBG spectra. Dominated by the emission from massive O and B stars, the overall shape of the UV continuum is modified shortward of Ly α by a decrement due to inter-galactic HI absorption. Several different sets of UV features are marked: stellar photospheric and wind, interstellar low- and high-ionization absorption, nebular emission from H II regions, Si II* fine-structure emission whose origin is ambiguous, and emission and absorption due to interstellar HI (Ly α and Ly β). There are numerous weak features which are not marked, as well as several features bluewards of Ly α which only become visible by averaging over many sightlines through the IGM. The composite LBG spectrum is available in electronic form from <http://www.astro.caltech.edu/~aes/lbgspec/>.

"BZK": Selects for both star-forming and "passive" galaxies at high z



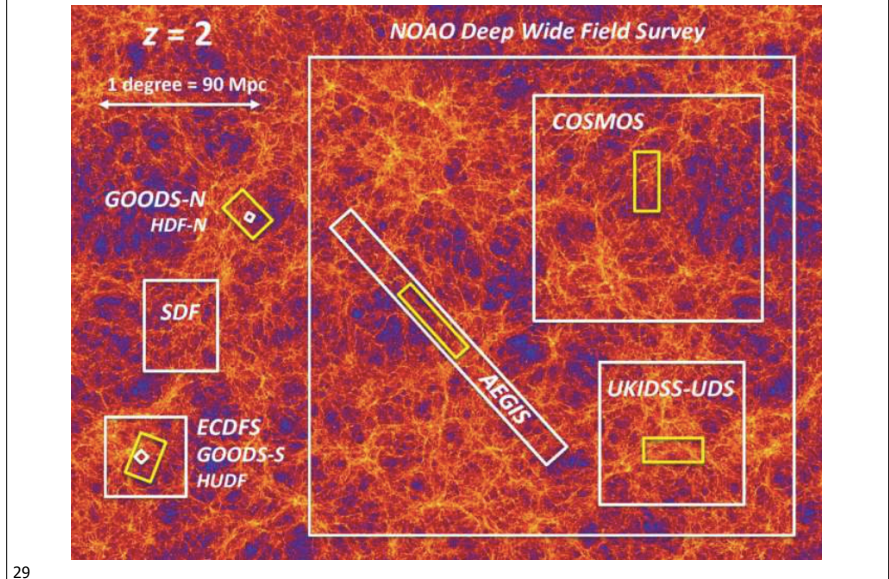
Can detect non-SF galaxies, and obscured SF galaxies with high SFRs

Introduced by
Daddi et al 2004

Strategies for Measuring Galaxy Evolution

- Broad population studies at a range of redshifts, by tracking 1 or more properties
 - Luminosity function evolution
 - Stellar mass function evolution
 - SFR evolution
 - SFR vs stellar mass evolution
- Tracking specific sub-populations through time
 - Red ("passive") and blue ("sf") sequences
 - Abundance matching

Some major surveys



A few technical points before results:

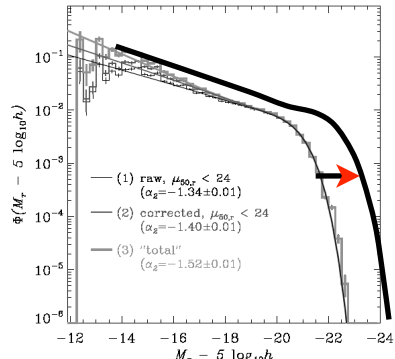
Types of Evolution

Separating star forming and
“passive” galaxies

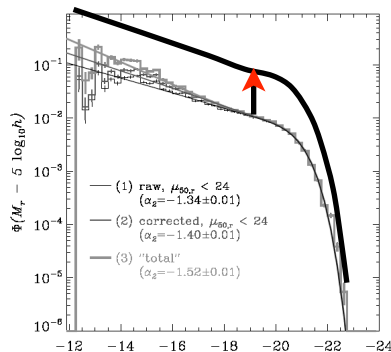
Abundance matching techniques

30

1. Two broad classes of evolution



Luminosity Evolution:
All galaxies brighter

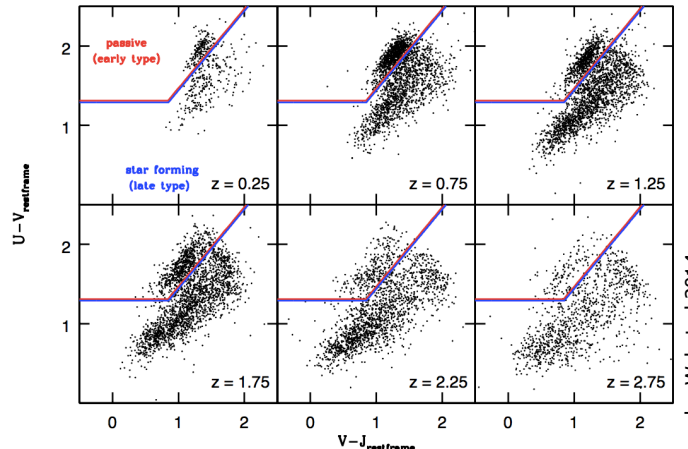


Density Evolution:
More galaxies at
each luminosity

31

Reality? Far more complex

2. Separating SF from Passive galaxies



Use bimodality w/ appropriate color cuts,
being careful about dust

32

3. Matching galaxies across cosmic time

- Abundance matching

Assume brightest galaxies at each redshift live in the most massive halos (gives M_{star} vs M_{halo})

- “Halo Occupation Distributions”

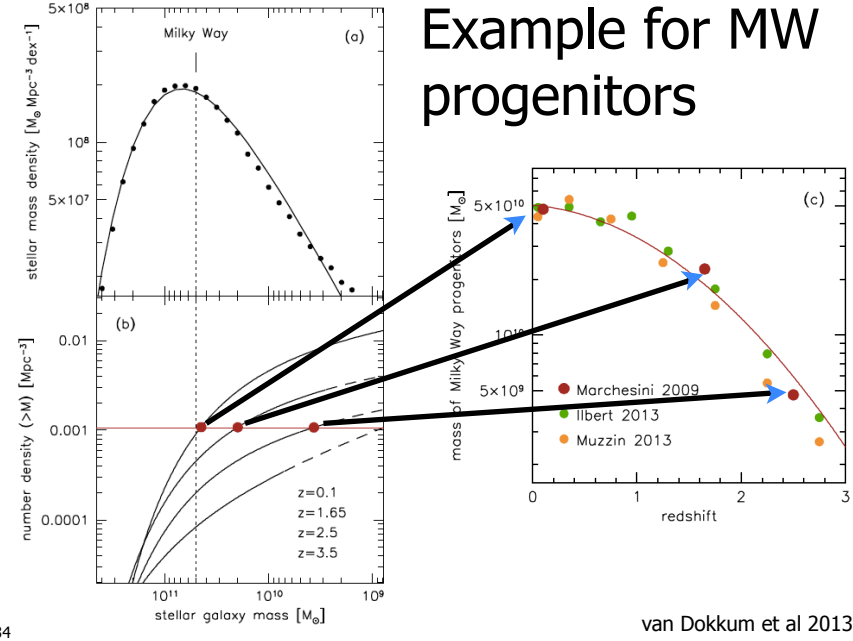
Match samples with identical correlation properties at each redshift (i.e. same comoving # density)

Assumes rank order is conserved, or that breaking rank is unimportant on average

33

(i.e., which galaxies at $z>1$ are progenitors of MW? of giant ellipticals, etc?)

Example for MW progenitors



van Dokkum et al 2013

Abundance Matched MW Progenitors

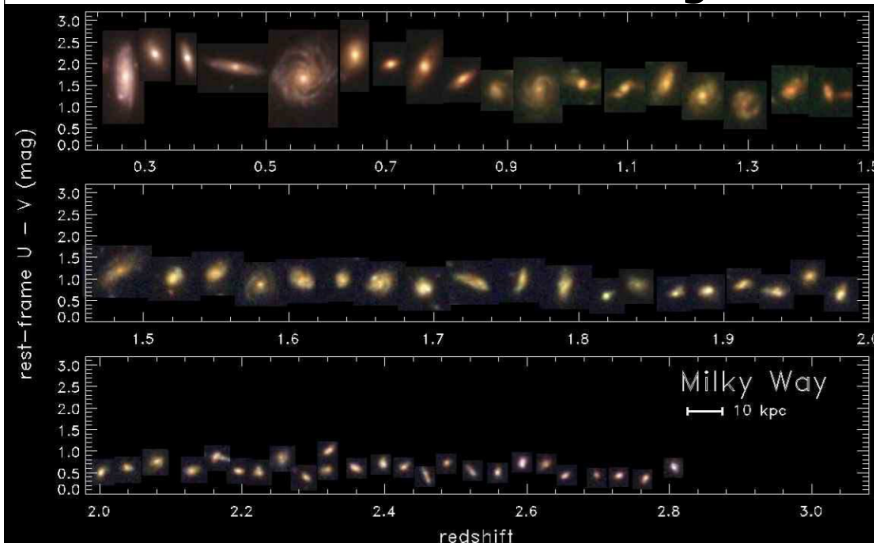
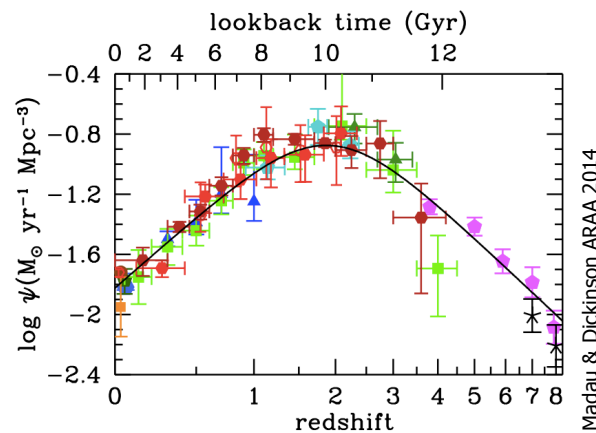


Figure 13. Examples of progenitors of an M31-mass galaxy from $z = 3$ to $z = 0.5$. Each galaxy is selected such that it has the approximate median $(U-V)$ and $V-J$ color derived for all progenitors in a given redshift bin (see Table 3). Each false-color image shows the approximate rest-frame U, R, V, J, H, I , and K bands (blue, green, red, respectively) using the ACS ($B_{432}/V_{606}/R_{700}$) and WFC3 ($J_{705}/H_{710}/I_{770}$) band closest to rest-frame UBV at each redshift. For this reason we do not show the K band for $z < 1.5$. The colors are measured at the same redshift as the progenitor stellar mass. The colors are corrected for extinction (using the method of Geringer et al. 2011; Kreckel et al. 2011). The images are plotted at their measured rest-frame $U-V$ color and redshift (slight adjustments in redshift are made for display purposes, but the rank order of the galaxies is unchanged). The image sizes are scaled to the same fixed physical scale where the most shows a scale of 10 kpc.

Papovich et al 2015

1. Star formation rate peaked sometime around $z=2$ -ish

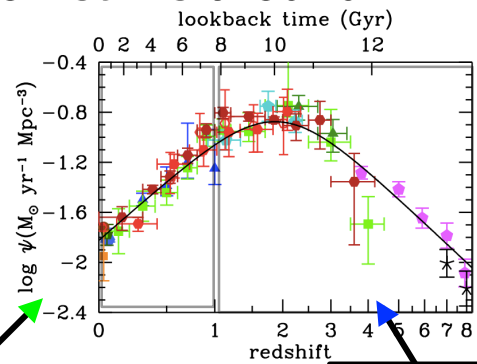


Madau & Dickinson ARAA 2014

- Lots of uncertainties in extinction corrections, conversion to SFR, etc

36

1. Star formation rate peaked sometime around $z=2$ -ish



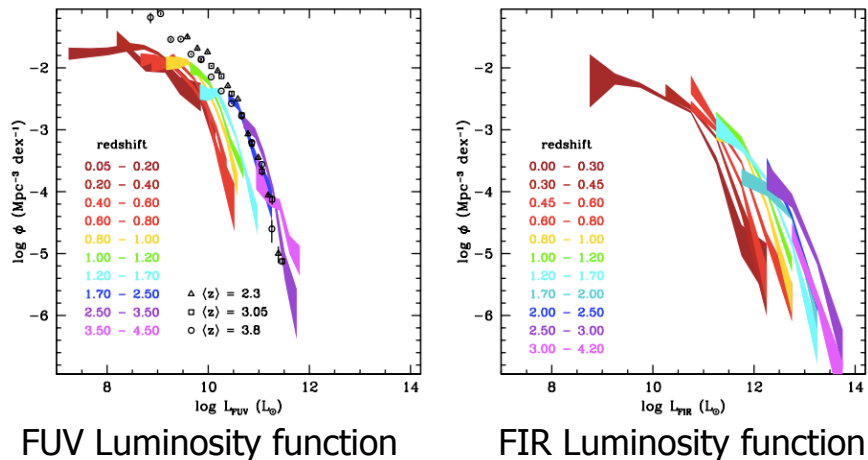
37

Late epoch of more quiescent evolution of disks & bulges

Initial epoch of rapid merging
Mimics DM merging rates

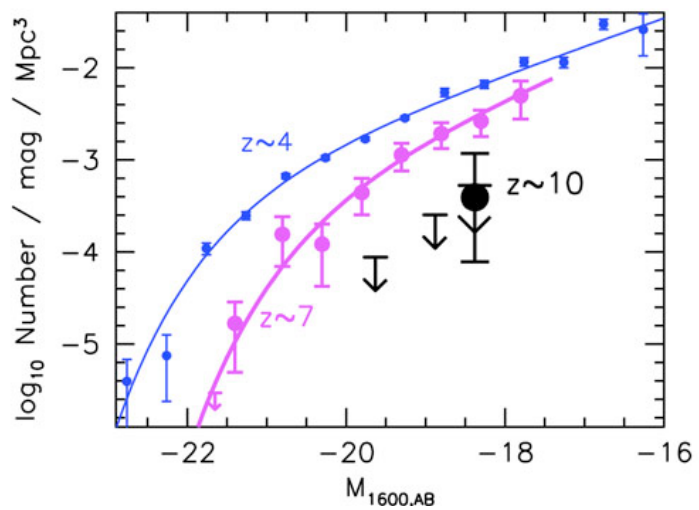
Madau & Dickinson ARAA 2014

1a. Associated with rapid evolution of UV and FIR luminosity



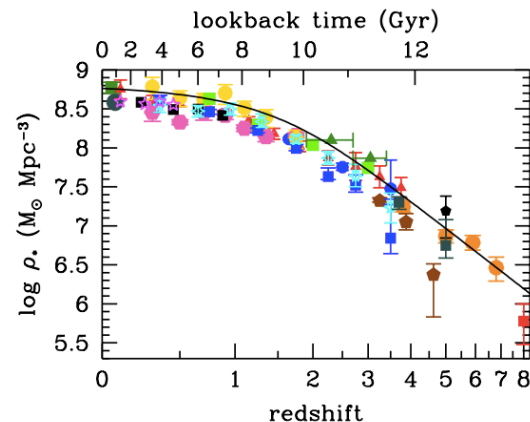
38 Madau & Dickinson ARAA 2014

2. Galaxy density evolves rapidly at early times



39

3. Stellar Mass of Universe has doubled since $z \sim 1-1.5$

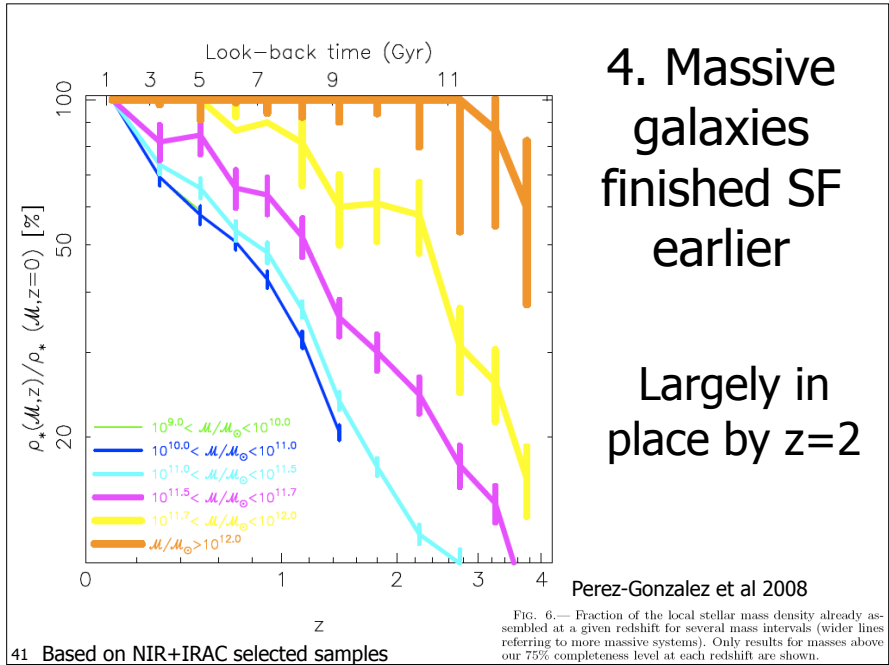


Madau & Dickinson ARAA 2014

Integrated SFR predicts somewhat more stellar mass today than we see

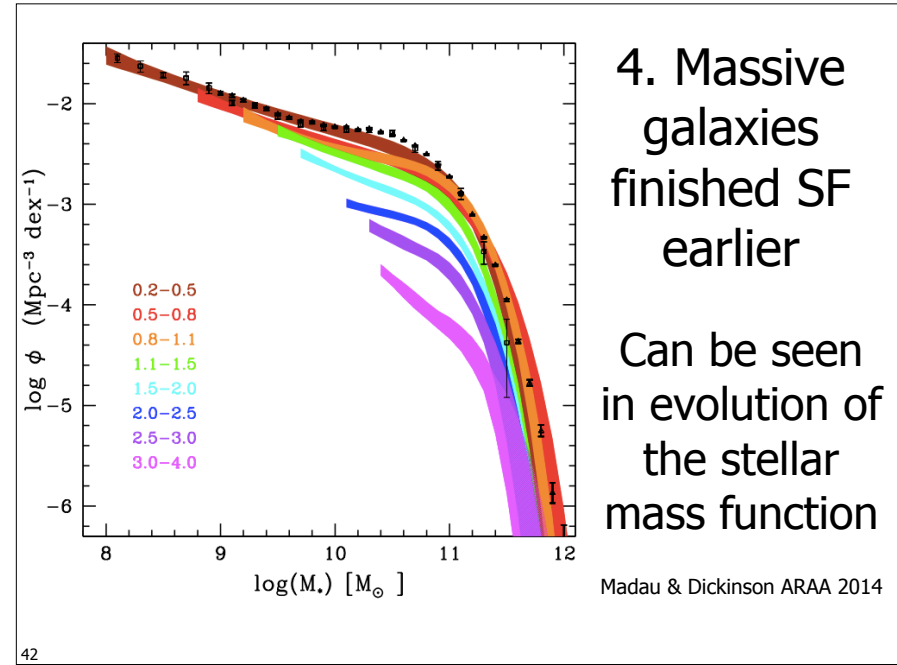
But, lots of possible sources of bias

Figure 11: The evolution of the stellar mass density. The data points with symbols are given in Table 2. The solid line shows the global stellar mass density obtained by integrating the best-fit instantaneous star-formation rate density $\psi(z)$ (Equations 2 and 10) with a return fraction $R = 0.27$.



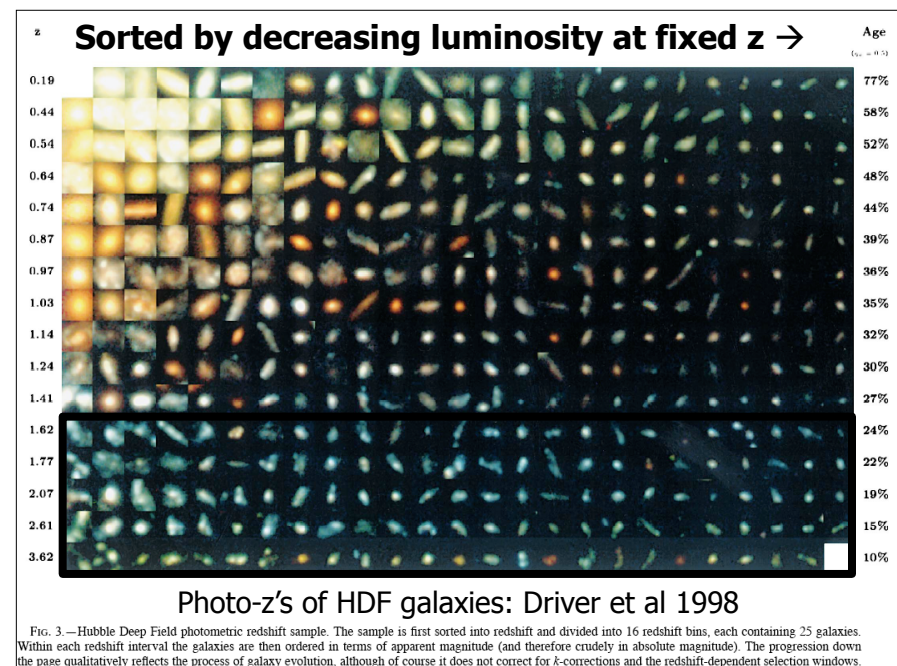
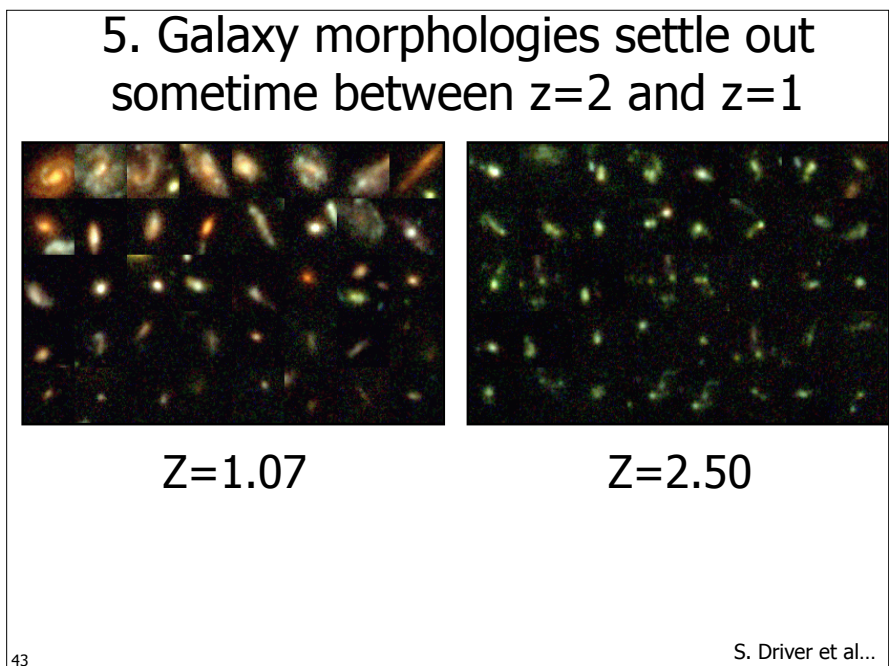
4. Massive galaxies finished SF earlier

Largely in place by $z=2$

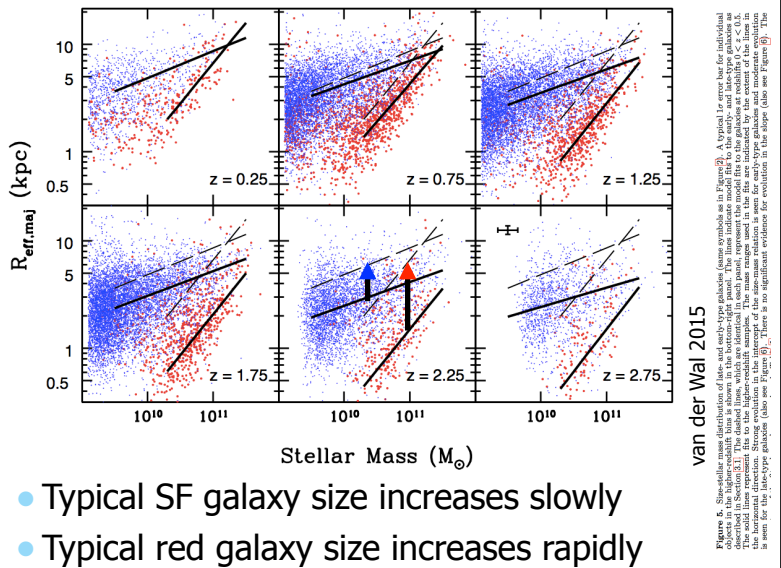


4. Massive galaxies finished SF earlier

Can be seen in evolution of the stellar mass function



6. The sizes of galaxies grow with time



45

Figure 6. Size-mass relations are illustrated for red and blue-type galaxies (from symbols as in Figure 9). A typical I Team-based model is applied to the observed data points. The line indicates the model fit to the red and blue-type galaxies as described in the bottom-right panel. The dashed lines, which are identical in each panel, represent the model fits to the red and blue-type galaxies at redshifts 0, z = 0.5, 1.5, and 2.5. The horizontal arrows, which are identical in each panel, represent the model fits to the red and blue-type galaxies at redshifts 0.25, z = 0.75, 1.25, and 1.75. The vertical arrows, which are identical in each panel, represent the model fits to the red and blue-type galaxies at redshifts 2.25 and 2.75. Strong evolution in the intercept of the size-mass relation is seen for early-type galaxies and moderate evolution in the slope (also see Figure 9). There is no significant evidence for evolution in the slope (also see Figure 9). The color bar indicates the median n_{Sersic} value for the sample.

8. Galaxies move onto the red sequence after $z \sim 1$ - 2 (?)

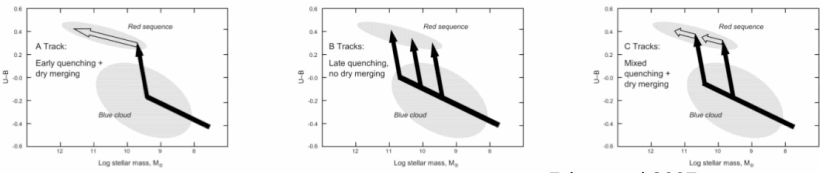


Figure 10. Schematic arrows showing galaxies migrating to the red sequence under different versions of the merging hypothesis. Evolutionary tracks are plotted in the color-mass diagram. Here it is assumed that red galaxies arise from blue galaxies when star formation is quenched during a major merger, causing the galaxy to double its mass, but the exact nature of the quenching mechanism is not crucial. Quenching tracks are shown by the nearly vertical black arrows. The mergers would be gas-rich ("wet") because the progenitor galaxies are blue objects making stars and hence contain gas. Once a galaxy arrives on the red sequence, it may evolve more slowly along it through a series of gas-poor, or "dry," mergers. These are shown as the white arrows. They are tilted upward to reflect the aging of the stellar populations during the more gradual dry merging. A major variable is the time of mass assembly vs. the time of quenching. Three possibilities are shown. Track A represents very early quenching while the fragments of the galaxy are still small. In that case, most mass assembly occurs in dry mergers along the red sequence. Track B is the other extreme having maximally late quenching. In that case, galaxies assemble most of their mass while still blue and then merge once to become red with no further dry merging. Track C is intermediate, with contributions from both mechanisms. This "mixed" scenario best matches the properties of both distant and local ellipticals. In addition to the merging scenario illustrated here, the gas supply of some disks may simply be choked off or stripped out without mergers, to produce diskless SOs. Such tracks would be vertical, but aside from their histories are similar. SOs dominate on the red sequence below L^* , ellipticals above (Marinoni et al. 1999).

- Many possible routes to evolution onto red sequence
- Important to test for consistency with entire population

47

7. A star forming blue sequence exists out to $z \sim 1$ - 2

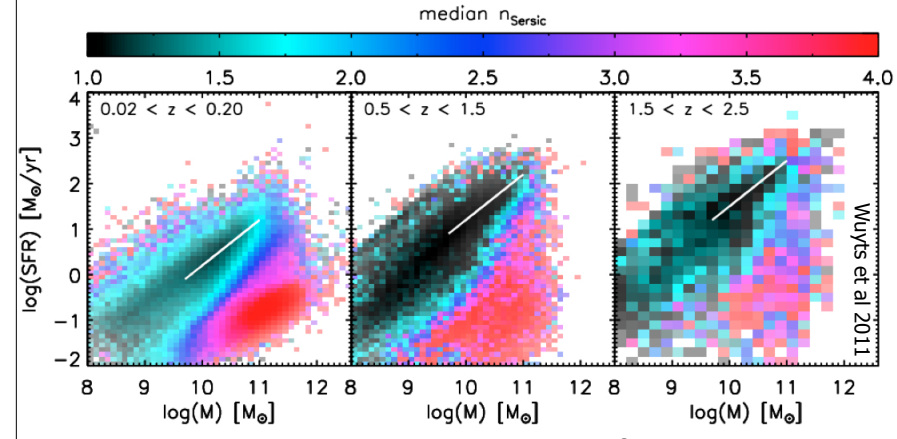


Figure 7. Surface brightness profile shape in the Star formation rate - Mass diagram. A structurally distinct "main sequence" of star-forming galaxies is clearly present at all observed epochs, and well approximated by a constant slope of 1 and a zero point that increases with lookback time (white line). While star-forming galaxies on the main sequence are well characterized by exponential disks, quiescent galaxies at all epochs are better described by cuspier, De Vaucouleurs profiles. Galaxies that occupy the tip and upper envelope of the main sequence also have cuspler light profiles, intermediate between main sequence galaxies and red and dead systems.

Narrowness of sequence suggests bursts of SF are not dominant form of mass growth (Noeske et al 2007)

9. Out to $z \sim 1$ - 2 , the red sequence galaxies are morphologically $n=4$

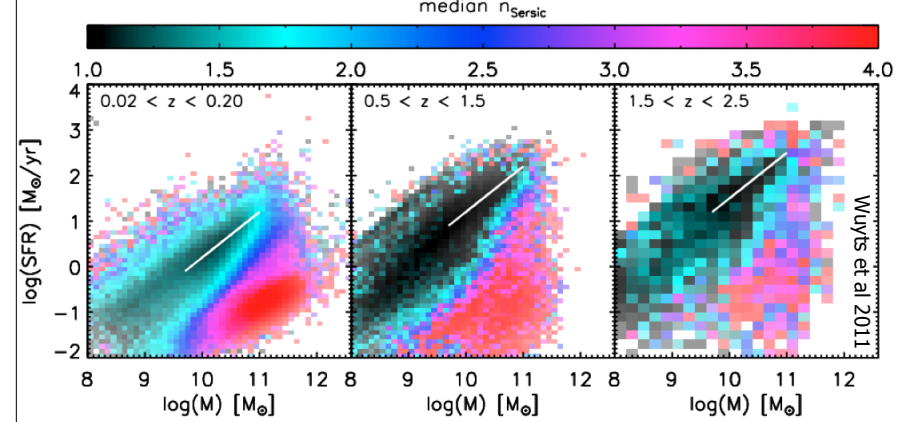
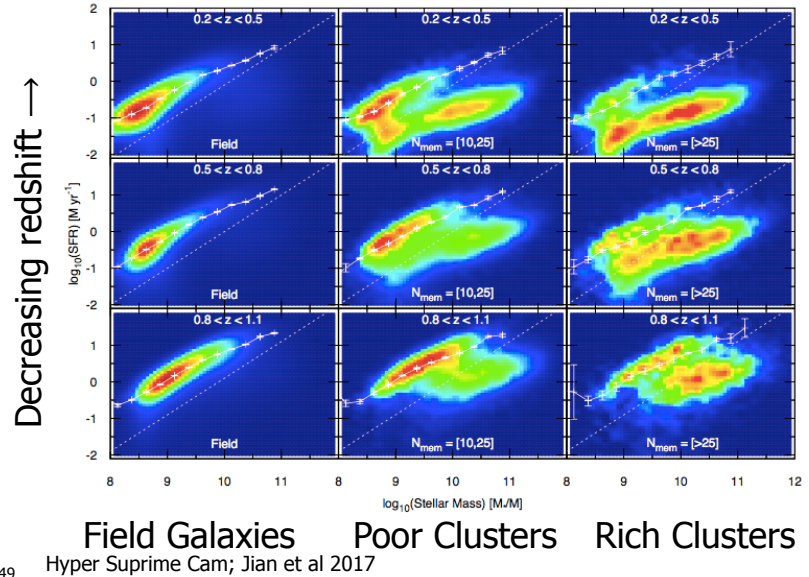


Figure 8. Surface brightness profile shape in the Star formation rate - Mass diagram. A structurally distinct "main sequence" of star-forming galaxies is clearly present at all observed epochs, and well approximated by a constant slope of 1 and a zero point that increases with lookback time (white line). While star-forming galaxies on the main sequence are well characterized by exponential disks, quiescent galaxies at all epochs are better described by cuspier, De Vaucouleurs profiles. Galaxies that occupy the tip and upper envelope of the main sequence also have cuspler light profiles, intermediate between main sequence galaxies and red and dead systems.

Narrowness of sequence suggests bursts of SF are not dominant form of mass growth (Noeske et al 2007)

10. Evolution varies w/ environment



49

Big issues

Much of the evolution appears set by the galaxy halo mass.

Why?

What are the roles of AGN feedback (& black hole growth) and why are they coupled to galaxy halo mass?

Why exactly does feedback shut down SF?

Different evolution of “centrals” and “satellites”

50